A Novel Heme-Degrading Enzyme that Regulates Heme and Iron Homeostasis and Promotes Virulence in *Enterococcus faecalis*

Debra N. Brunson[1], Hader Manzer[2], Alexander B. Smith[2], Joseph P. Zackular[2, 3, 4], Todd Kitten[5], José A. Lemos[1]*

[1]Department of Oral Biology, University of Florida College of Dentistry, Gainesville, FL, USA

[2] Division of Protective Immunity, Children's Hospital of Philadelphia, Philadelphia, Pennsylvania, USA

[3] Department of Pathology and Laboratory Medicine, Perelman School of Medicine, University of Pennsylvania, Philadelphia, Pennsylvania, USA

[4] Center for Microbial Medicine, Children's Hospital of Philadelphia, Philadelphia, PA, USA

[5] Department of Oral and Craniofacial Molecular Biology, Philips Institute for Oral Health Research, School of Dentistry, Virginia Commonwealth University, Richmond, VA 23298-0566, USA

Running title: Heme degradation in *E. faecalis*

*** Correspondence:** jlemos@dental.ufl.edu

ABSTRACT

Enterococcus faecalis, a gut commensal, is a leading cause of opportunistic infections. Its virulence is linked to its ability to thrive in hostile environments, which includes host-imposed metal starvation. We recently showed that *E. faecalis* evades iron starvation using five dedicated transporters that collectively scavenge iron from host tissues and other iron-deprived conditions. Interestingly, heme, the most abundant source of iron in the human body, supported growth of a strain lacking all five iron transporters (Δ5Fe). To release iron from heme, many bacterial pathogens utilize heme oxygenase enzymes to degrade the porphyrin that coordinates the iron ion of heme. Although *E. faecalis* lacks these enzymes, bioinformatics revealed a potential ortholog of the anaerobic heme-degrading enzyme anaerobilin synthase, found in *Escherichia coli* and a few other Gram-negative bacteria. Here, we demonstrated that deletion of OG1RF_RS05575 in *E. faecalis* (ΔRS05575) or in the Δ5Fe background (Δ5FeΔRS05575) led to intracellular heme accumulation and hypersensitivity under anaerobic conditions, suggesting *RS05575* encodes an anaerobilin synthase, the first of its kind described in Gram-positive bacteria. Additionally, deletion of *RS05575*, either alone or in the Δ5Fe background, impaired *E. faecalis* colonization in the mouse gastrointestinal tract and virulence in mouse peritonitis and rabbit infective endocarditis models. These results reveal that RS05575 is responsible for anaerobic degradation of heme and identify this relatively new enzyme class as a novel factor in bacterial pathogenesis. Findings from this study are likely to have broad implications, as homologues of *RS05575* are found in other Gram-positive facultative anaerobes.

IMPORTANCE

Heme is an important nutrient for bacterial pathogens, mainly for its ability to serve as an iron source during infection. While bacteria are known to release iron from heme using enzymes called heme oxygenases, a new family of anaerobic heme-degrading enzymes has been

52 described recently in Gram-negative bacteria. Here, we report the first description of anaerobic
53 heme degradation by a Gram-positive bacterium, the opportunistic pathogen *Enterococcus*
54 *faecalis*, and link activity of this enzyme to their ability to colonize and infect the host. We also
55 show that homologues of this enzyme are found in many Gram-positive facultative anaerobes,
56 implying that the ability to degrade heme under anaerobic conditions may be an overlooked
57 fitness and virulence factor of bacterial pathogens.
58

INTRODUCTION

Enterococcus faecalis is a facultative anaerobe known for its intrinsic multi-stress resiliency and ability to cause numerous opportunistic infections (1). However, *E. faecalis* is also a member of the gut microbiota and will typically only cause disease under specific conditions that include, but are not limited to, extended antibiotic usage, compromised immunity, and utilization of indwelling medical devices (2). For the most part, the virulence of *E. faecalis* derives from its inherent capacity to overcome various stress conditions, form biofilms on both biotic and abiotic surfaces, and subvert immune responses (3). Regarding the latter, a central aspect of the innate immune response of enterococcal hosts involves the rapid mobilization of proteinaceous metal chelators to the site of infection that avidly bind to trace metals such as iron, manganese and zinc, a process known as nutritional immunity (4-7).

An essential trace metal to virtually all forms of life, iron holds a prominent role in bacterial physiology and in host-pathogen interactions as its electrochemical properties and abundance in nature makes it the preferred redox cofactor for enzymatic reactions (8). We recently showed that *E. faecalis* can efficiently scavenge iron from the environment via the cooperative activity of three highly conserved and two novel iron transporters (9). The simultaneous inactivation of all five transporters (Δ5Fe strain) resulted in major growth impairment under iron-depleted conditions, which, as expected, was accompanied by a substantial reduction in intracellular iron pools. However, the virulence potential of the Δ5Fe strain in animal models varied depending on the type of model (the invertebrate *Galleria mellonella* larvae or mice) and, in the case of mice, the infected site. Specifically, virulence of Δ5Fe was significantly attenuated in *G. mellonella*; however, the Δ5Fe strain showed impaired capacity to infect the peritoneal cavity while it disseminated and infected spleens as well as the parental strain. We suspected that these differences correlate with heme availability, as heme—plentiful in blood and mammalian tissues—serves as a major source of iron for some of the most successful bacterial pathogens (10-13). Furthermore, non-hematophagous insects like *G.*

mellonella are virtually heme-free, as they use two copper ions coordinated by histidine residues to transport oxygen rather than the hemoglobin/Fe-heme complexes found in vertebrates (14). As anticipated, heme supplementation restored growth and intracellular iron homeostasis in the Δ5Fe strain grown in media lacking any other type of iron source while injection of small amounts of heme into the *G. mellonella* hemocoel restored virulence of Δ5Fe to levels comparable to those of the parent strain (9). While these results clearly demonstrate that *E. faecalis* can utilize heme as an iron source, the mechanisms by which it acquires heme from the environment—since enterococci cannot synthesize heme (15, 16)—and how the iron ion is released from the porphyrin ring remain unknown.

Oxidative degradation mediated by heme oxygenases is the best described mechanism of heme degradation in bacteria (17). In important and diverse bacterial pathogens such as *Streptococcus pyogenes* and *Pseudomonas aeruginosa*, the canonical HO-1 heme oxygenase uses oxygen to disrupt the tetrapyrrole ring to liberate biliverdin, CO_2 and Fe^{+2} (17, 18). Additionally, some bacteria encode the so-called non-canonical heme oxygenase, such as the *Staphylococcus aureus* IsdG/I, which uses oxygen to degrade heme into staphylobilin and formaldehyde (19-21). Recently, an oxygen-sensitive radical S-adenosylmethionine methyltransferase (rSAM), named ChuW, was identified in *Escherichia coli*, and shown to degrade heme's porphyrin ring under anaerobic conditions (22). ChuW utilizes a primary carbon radical S-adenosylmethionine to promote methyl transfer and subsequent linearization of the porphyrin ring, releasing the iron atom and the linear tetrapyrrole product anaerobilin, hence the designation anaerobilin synthase (22, 23). Aside from *E. coli*, ChuW homologues have been described in *Vibrio cholerae* and *Fusobacterium nucleatum* (22, 24, 25). Considering that either canonical or non-canonical heme oxygenases cannot function under anaerobic conditions, the presence of an oxygen-independent enzyme that mediates heme degradation is expected to provide a competitive advantage for bacteria that inhabit anaerobic environments.

Through bioinformatic analysis, we identified a ChuW ortholog in the *E. faecalis* OG1RF genome. Further analysis indicated that OG1RF_RS05575 (hereafter referred to as RS05575) is conserved across the *Enterococcus* genus as well as other facultative anaerobic Gram-positive cocci (26). In this investigation, we provide the first insights into the mechanisms of anaerobic heme degradation in Gram-positive bacteria and, for the first time, link the activity of an anaerobilin synthase with bacterial virulence.

RESULTS

***Enterococcus faecalis* internalizes and utilizes heme as an iron source.** We recently showed that *E. faecalis* utilizes heme as an iron source while others have shown that it will grow to higher cell density and form more robust biofilms in the presence of heme (9, 27). To further explore the relationship between heme and iron in *E. faecalis*, we tested whether heme supplementation could hinder elemental iron uptake. To do so, *E. faecalis* OG1RF was grown to mid-log phase in a chemically-defined medium, FMC, lacking an iron source (28). Then, mid-log grown cultures were divided into aliquots and supplemented with either 1µM ^{55}Fe (control), 1µM ^{55}Fe + 10µM heme, or 1µM ^{55}Fe + 40µM $FeSO_4$ with samples taken after 1 and 5 minutes. As expected, the addition of cold (unlabeled) $FeSO_4$ effectively slowed ^{55}Fe uptake with ~70% reduction after 5 minutes when compared to the control sample (Fig 1A). Heme was also effective, seemingly more than $FeSO_4$, as it reduced ^{55}Fe uptake by ~90% after the same period (Fig 1A). As we have shown that transcription of the iron transporters *efaABC*, *emtABC*, *feoAB, fhuDCBG* and *fitABCD* was significantly elevated during iron starvation (9), we next asked if heme supplementation could shut down this activation. Indeed, heme treatment lowered transcription of *feoB* (~3-fold), *fitA* (~15-fold), *fhuB* (~13-fold), and *emtB* (~1.5-fold) (Fig 1B). However, heme treatment led to ~100-fold increase in *efaA* expression (Fig 1B). Because *efaCBA* codes for a dual iron/manganese transporter, we wondered if this induction was

necessary to enhance manganese uptake to mitigate heme toxicity and assure maintenance of a balanced iron:manganese ratio. To investigate this possibility, we assessed *mntH2* levels, the other major manganese transporter of *E. faecalis* (29) and of the heme efflux pump *hrtA* (30). As predicted, *mntH2* levels were 10-fold higher after heme treatment while *hrtA* was induced by approximately 100-fold (Fig 1B). Finally, we determined intracellular heme content of OG1RF cultures grown in FMC supplemented with 20µM heme +/- 10µM $FeSO_4$. We found that when grown with both heme and $FeSO_4$, intracellular heme levels nearly doubled (~73% increase) compared to cells grown only in heme indicating that *E. faecalis* will slow down heme degradation when free iron is available (Fig 1C). Collectively, these results provide unequivocal evidence that *E. faecalis* can rapidly import and then degrade heme to release the iron ion.

Identification of an oxygen-sensitive heme-degrading enzyme in *E. faecalis*. To serve as an iron source, the porphyrin ring of heme must be degraded. In bacteria, oxidative degradation is often mediated by enzymes called heme oxygenase. *In silico* analysis indicate that enterococcal genomes do not encode heme oxygenases (26) but, on the other hand, identified an ortholog of *E. coli* ChuW (gene ID: OG1RF_RS05575). ChuW is an oxygen-sensitive, r-SAM-type enzyme, that catalyzes the degradation of heme into a linear tetrapyrrole named anaerobilin (23). Even though the similarity between ChuW and RS05575 appears unremarkable (23% identity and 44.5% similarity), the CXXXCXXC r-SAM motif essential for binding of S-adenosylmethionine and an aspartic acid residue critical for ChuW activity (23) are conserved in RS05575, with several other important residues identified in ChuW and few other anaerobilin synthases characterized to date being also present in RS05575 (Fig 2B). Despite this moderate similarity at the amino acid level, superimposition of AlphaFold2 predicted structures of *E. coli* ChuW and *E. faecalis* RS05575 revealed a striking structural similarity between the two proteins (Fig 2C). Using a pairwise structure alignment tool from the Research Collaboratory for Structural Bioinformatics (RCSB) Protein Data Bank (31), we derived analytical

scores to demonstrate the structural similarity of ChuW and RS05575 with a root mean square deviation score of 3.01 and a template modeling score of 0.78. Using the AlphaFold server and the HeMoQuest webserver to predict potential ligand interactions, we found that RS05575 likely binds heme using Y7, C20, Y59, Y190, Y236, and/or H250 as coordinating residues (Fig S1). Analysis of all genome sequences available at the Bacterial and Viral Bioinformatic Resource Center (BV-BRC) (26) indicated that RS05575 is widespread among enterococci and members of the Enterococcaceae family (Fig 3 and Table S1). Notably, RS05575 orthologs with ~70% similarities are found in several facultative Gram-positive anaerobes, including streptococcal and staphylococcal species.

Inactivation of RS05575 differentially affects growth of *E. faecalis* under aerobic and anaerobic conditions. To explore the biological significance of RS05575, we generated a RS05575 deletion (ΔRS05575) and genetically complemented (ΔRS05575c) strains. We assessed growth of ΔRS05575 in FMC medium originally prepared without an iron source (FMC[-Fe]) and then supplemented with either 20 µM heme (FMC[+heme]) or 20 µM $FeSO_4$ (FMC[+Fe]). As we expected RS05575 to be only active under anaerobiosis, we assessed the capacity of ΔRS05575 to grow under both aerobic and anaerobic conditions. For the latter, we used FMC retaining dissolved oxygen (herein FMC_{DO}) as well as O_2-purged media (FMC_{O2P}). In FMC[-Fe], the ΔRS05575 strain grew as well as the parent, reaching slightly higher growth yields under the more strict (FMC_{O2P}) anaerobic condition (Fig 4A-C). Similar results were obtained in FMC[+Fe] as the mutant reached higher final growth yields under anaerobiosis (Fig 4D-F). In FMC[+heme], ΔRS05575 strain grew similarly to the parent strain reaching higher growth yields when incubated in air but not in FMC_{DO} (Fig 4G-H). Notably, both the OG1RF parent and ΔRS05575 strains struggled to grow in the presence of heme under strict (FMC_{O2P}) anaerobic conditions. Specifically, OG1RF grew very poorly with an extended lag phase of ~12

hours while the ΔRS05575 strain failed to grow (Fig 4I). Genetic complementation restored all relevant growth phenotypes to parental levels (Fig 4C, G and I) of ΔRS05575.

Inactivation of RS05575 leads to heme accumulation in microaerophilic and anaerobic environments. To investigate the role of RS05575 in heme catabolism, we quantified intracellular heme in the OG1RF and ΔRS05575 strains grown to mid-log phase in FMC[-Fe] supplemented with 20 μM heme under an oxygen gradient (see methods and Fig 5A for details) While dissolved oxygen levels had no impact on heme pools in OG1RF, intracellular heme nearly doubled in ΔRS05575 grown under low oxygen (static with no headspace) or anaerobic conditions (Fig 5B). Genetic complementation reversed this phenotype (Fig 5C).

To further define the role of RS05575 in heme degradation and its importance to iron homeostasis, we leveraged the extreme iron starvation that can be imposed to the Δ5Fe strain by growing cells in iron-depleted media (9). Specifically, we generated a sextuple mutant by introducing the RS05575 deletion into the Δ5Fe background and used the original Δ5Fe as well as the ΔRS05575 and Δ5FeΔRS05575 strains to compare their heme uptake and degradation efficiency. When compared to Δ5Fe, the Δ5FeΔRS05575 strain grew equally well in different oxygen content under iron-starving conditions or in media supplemented with either $FeSO_4$ or heme (Fig. S1A-I). However, different than ΔRS05575, the Δ5FeΔRS05575 strain grew in FMC_{O2P}[+heme] albeit still displaying an extended lag phase. The reason for this unexpected observation remains to be determined.

Upon identifying conditions that supported growth of all strains, we next monitored their heme uptake capacity by growing cells to mid-log phase in FMC_{O2P}[-Fe], spiked cultures with 10μM heme, and monitored intracellular heme content 5, 15, and 60 minutes after heme treatment. As expected based on prior evidence that the Δ5Fe strain is primed to take up heme (9), both Δ5Fe and Δ5FeΔRS05575 acquired heme much more rapidly than the OG1RF and ΔRS05575 strains (Fig 6A, notable differences at $T_{15\text{-min}}$). To monitor heme degradation, we set

up another experiment where cultures were spiked with 10 µM heme for 15 minutes, the cells collected by centrifugation, washed in PBS once, and suspended in fresh FMC_{O2P}[-Fe] with intracellular heme monitored for up to 3 hours. While intracellular heme continued to increase in both OG1RF and ΔRS05575 during the first hour after media change, likely due to residual uptake of heme bound to the cell surface, it declined by ~35% in OG1RF after 3 hours while remaining steady in ΔRS05575 (Fig 6B). Most importantly, heme levels sharply decreased (~65%) in the Δ5Fe strain after 3 hours but not in Δ5FeΔRS05575. Collectively, these results strongly support that RS05575 mediates anaerobic heme degradation (Fig 6B).

RS05575 plays a role in *E. faecalis* virulence and intestinal colonization. Upon demonstration that RS05575 mediates heme degradation under anaerobic conditions, we sought to investigate its possible role in enterococcal fitness and pathogenesis. Given the close association between heme and iron homeostasis, we conducted the following series of experiments using the ΔRS05575, Δ5Fe, and Δ5FeΔRS05575 strains. First, we used an intra-peritoneal challenge mouse model, in which *E. faecalis* spreads systemically within 24 hours. As shown previously (9), the ability of the Δ5Fe strain to infect the peritoneal cavity was impaired (~1-log reduction) when compared to OG1RF but not in the (heme-rich) spleen (Fig 7A-B). We also showed that the Δ5Fe strain could efficiently colonize the heart and liver but not the kidney (Fig 7C-E). The ΔRS05575 single mutant displayed defective ability to infect the peritoneal cavity, liver and kidney, but not spleen or heart. Finally, virulence of Δ5FeΔRS05575 was attenuated in all tissues sampled and was the only mutant recovered at significantly lower numbers from spleens and hearts when compared to the OG1RF parent strain (Fig 7).

Next, we used the rabbit infective endocarditis (IE) model to determine if RS05575 also plays a role in enterococcal IE and, in parallel, assess the virulence of the Δ5Fe strain in this life-threatening infection. Briefly, upon creation of a sterile vegetation of the heart endothelium, the animals were systemically infected with an inoculum containing equal amounts of OG1RF,

ΔRS05575, Δ5Fe, and Δ5FeΔRS05575 strains, and the percentage of each strain recovered from infected heart vegetations assessed 24-hours post-infection (Fig 8A). The Δ5Fe (~12%) and Δ5FeΔRS05575 (less than 5%) strains were recovered at significantly lower rates when compared to OG1RF (~48%) (Fig 8B). The ΔRS05575 strain was also recovered at lower rates (~30%) but this difference was not statistically significant when compared to OG1RF.

In the final set of experiments, we evaluated the importance of iron scavenging and RS05575 to the ability of *E. faecalis* to colonize its natural habitat, the mammalian gut. For this, we used a mouse model (32, 33) in which the gut flora is depleted with antibiotics prior to oral gavage with individual strains (Fig 9A). Strain fitness was determined by enumeration of bacteria recovered from feces 1, 2 and 3 days post-gavage (See Fig 9A and methods for details). When compared to animals infected with OG1RF, we observed significant decreases in the recovery of all three mutants over time, with the sextuple mutant showing the largest defect (Fig 9B). These studies collectively demonstrate that RS05575 enhances enterococcal fitness and virulence within the host, implicating, for the first time, anaerobic heme degradation in bacterial pathogenesis.

DISCUSSION

In bacteria, heme serves both as a nutrient cofactor and as an iron source. However, when in excess, it disrupts the cellular membrane, triggers DNA damage, and oxidizes lipids (34). To maintain heme homeostasis, bacteria evolved different mechanisms to acquire, export, synthesize, degrade, and sequester heme (13, 35). While several of these mechanisms have been identified and characterized in other Gram-positive pathogens, little is known about the mechanisms utilized by enterococci to acquire, utilize and maintain heme homeostasis (26, 34). Previously, we showed that iron starvation in *E. faecalis* can be fully reversed by heme supplementation (9). Here, we provided unequivocal evidence that heme serves as a major, if not the preferred, iron source for *E. faecalis* by showing that free iron uptake is inhibited by

heme supplementation. Furthermore, we showed that intracellular heme remains elevated when free iron is abundant, indicating that *E. faecalis* possesses dedicated, likely inducible, mechanisms to degrade and then use heme as an iron source. While the prevailing bacterial mechanism to degrade heme is through oxidative degradation, mediated by heme oxygenases (17, 36), extensive bioinformatic searches for the presence of these enzymes in enterococcal genomes failed to reveal potential candidates. Thus, it is possible that enterococci rely on a non-enzymatic mechanism, termed coupled oxidation, to degrade heme when in the presence of oxygen (26, 37, 38). For example, the respiratory pathogen *Streptococcus pneumoniae* has been shown to degrade heme via production of H_2O_2, a metabolic byproduct of pyruvate oxidase and lactate oxidase enzymatic reactions (37-39). While *E. faecalis* does not encode either of these enzymes, it is known to generate low amounts of H_2O_2 that can be enhanced when cells are grown on alternative sugars such as glycerol and galactose (40, 41).

While studies to elucidate the mechanisms of aerobic heme degradation and identify the mechanism(s) by which *E. faecalis* obtains heme from the environment are active areas of investigation in our laboratory, here we described the identification of RS05575, an enzyme that resembled *E. coli* ChuW. The discovery of ChuW unveiled a new paradigm for heme degradation that, due to the high oxygen sensitivity of this new class of enzyme, is anticipated to be restricted to facultative or strict anaerobes (22, 23, 25). Despite RS05575 annotation as a coproporphyrinogen synthase, an enzyme that catalyzes the conversion of coproporphyrinogen III to protoporphyrinogen IX, *E. faecalis* genomes lack the remaining biosynthetic operon for anaerobic heme synthesis. In fact, a homologue of RS05575 in *S. aureus* Newman strain (68% amino acid similarity with RS05575) was found to have no role in anaerobic heme biosynthesis (42). Leveraging the fact that the Δ5Fe strain heavily depends on heme to maintain iron homeostasis, we showed that even though Δ5Fe strains are primed for heme uptake, the accelerated heme degradation that is observed in Δ5Fe is completely lost in the sextuple Δ5FeΔRS05575 mutant under oxygen-depleted conditions. In agreement with the anticipated

oxygen-sensitivity of RS05575, we also found that RS05575 can only protect *E. faecalis* from heme toxicity under strict anaerobic conditions. Collectively, these studies reveal that RS05575 mediates heme degradation and is critical for heme homeostasis under anaerobiosis and, possibly, microaerophilic conditions.

Previously, we used the peritonitis model to demonstrate that the importance of iron scavenging transport systems to *E. faecalis* virulence was host niche dependent, and speculated that these tissue/organ-specific differences were linked to differences in heme bioavailability (9). Here, we followed up on these observations by revisiting the virulence potential of Δ5Fe in the peritonitis model while also testing the virulence potential of ΔRS05575 and Δ5FeΔRS05575. To further probe the proposed niche-specific association of iron and heme bioavailability with pathogenesis, we sampled additional organs by determining bacterial burden in livers, kidneys, and hearts homogenates. We confirmed the impaired (niche-dependent) virulence phenotype of the Δ5Fe strain that now includes evidence of impaired colonization of kidneys but no of other organs such as spleen (shown before), heart, or liver. Noteworthy, the ΔRS05575 and Δ5FeΔRS05575 strains also displayed impaired ability to colonize the kidney. Here, it should be noted that the kidney is highly susceptible to heme-iron injury and that HO-1 levels are elevated in kidneys to protect the organ from heme toxicity (43). In the end, the most relevant finding from these studies is that virulence of ΔRS05575 alone is attenuated and exacerbated when RS05575 is inactivated in the Δ5Fe background. In fact, only the sextuple Δ5FeΔRS05575 strain displayed significant defects in dissemination to spleen and heart and was the least fit strain in the competitive rabbit IE model. Similar trends were noted in the gut colonization mouse model whereby all mutants colonized the gut poorly when compared to the parent strain. In the future, it will be interesting to assess the virulence potential of these mutants in localized infections, such as wounds or urinary tract infections, and to test their ability to colonize the gut when levels of heme are elevated, whether from intake of a heme-rich diet or due to colitis (44, 45). As we observed fitness defects in the colonization of the polymicrobial

mouse gastrointestinal tract, it would also be compelling to determine how loss of RS05575, alone or in the Δ5Fe background, affects *E. faecalis* fitness and pathogenic behavior in polymicrobial biofilm infections.

While biochemical studies are still lacking, this study provides the first description of an active mechanism of anaerobic heme degradation in a Gram-positive bacterium. Moreover, it links, also for the first time, anaerobic heme degradation with bacterial colonization of the host and virulence. Because RS05575 orthologs are present in other Gram-positive bacteria, findings from this study provide the foundation for future studies that can establish a new paradigm for how other Gram-positive facultative anaerobes utilize heme and, at the same time, protect itself from heme toxicity under oxygen-depleted conditions.

MATERIALS AND METHODS

Bacterial strains and growth conditions. Bacterial strains used in this study are listed in Table 1. All *E. faecalis* strains were grown overnight aerobically at 37°C in BHI (Difco) unless otherwise noted. For controlled growth under metal-depleted conditions, we used the chemically defined FMC media originally developed for cultivation of oral streptococci (36), with minor modifications. The recipe for FMC is shown in Table S2. Specifically, the base media was prepared without any of the metal components (magnesium, calcium, iron, and manganese) and treated with Chelex (BioRad) to remove contaminating metals. The pH was adjusted to 7.0 and filter sterilized. All FMC component solutions were prepared using National Exposure Research Laboratory (NERL) trace metal grade water, filter sterilized, and then added to the media. Heme (Sigma-Aldrich) was prepared in 1.4 M NaOH in NERL trace metal grade water. Calcium, magnesium, manganese, iron, and heme were added at concentrations specified in the text or figure legend. For reverse transcriptase quantitative PCR (RT-qPCR) analysis, RNA was isolated from cells grown in FMC[-Fe] to OD_{600} of 0.4 and spiked with 20 µM heme with aliquots taken 0 and 60 minutes post-heme supplementation. To generate growth curves, cultures were

grown in FMC[-Fe] and diluted 1:200 into fresh FMC[-Fe] supplemented with heme and/or $FeSO_4$ as indicated in the text and figure legends. Aerobic cell growth was monitored using the Bioscreen growth reader (Oy Growth Curves). Growth of anaerobically grown cells was monitored in a 96-well plate reader (Byonoy) in an anaerobic chamber (Coy).

Construction of mutant strains. Markerless deletions of RS05575 in *E. faecalis* OG1RF were carried out using the pCJK47 genetic exchange system (46). Briefly, PCR products with ~1 kb in size flanking each coding sequence were amplified with the primers listed in Table S3. To avoid unanticipated polar effects, amplicons included either the first or last residues of the coding sequences. Cloning of amplicons into the pCJK47 vector, electroporation, and conjugation into *E. faecalis* strains and isolation of single mutant strains (ΔRS05575) were carried out as previously described (46). Isolation of Δ5FeΔRS05575 was done by conjugation of the pCJK47 vector with the Δ5Fe strain used in a previous publication (9). All gene deletions were confirmed by PCR sequencing of the insertion site and flanking region.

Construction of the complemented strains. The pCJK47 vector was used to insert RS05575 back into its original genetic loci to be regulated by the native promoter. Briefly, the coding sequence of RS05575 was amplified from OG1RF using the primers listed in Table S3. We used the In-fusion cloning system (Takara Bio) to generate the allelic exchange plasmid. The pCJK47 vector was digested with BamHI and PstI to yield pCJK47-RS05575c vector. Upon propagation in *E. coli* EC1000, pCJK47-RS05575c was electroporated into the conjugation strain *E. faecalis* CK111, and the plasmid mobilized into ΔRS05575 using a standard conjugation protocol (46).

366 **RNA analysis.** RNA was isolated from cells before and after exposure to 20 µM heme using the
367 PureLink™ RNA Mini Kit (Invitrogen). Genomic DNA (gDNA) was degraded using TURBO
368 Dnase kit (Invitrogen) and cDNA synthesis from 1 µg total RNA using the high-capacity cDNA
369 reverse transcription kit (Applied Biosystems). RT-qPCR was performed using iTaq Universal
370 SYBR supermix (BioRad) with primers listed in Table S3. Copy number was determined using a
371 standard curve generated from OG1RF genomic DNA (gDNA) and fold change calculated.
372
373 **Phylogenetic analysis.** ChuW and RS05575 amino acid sequences were compared using
374 Clustal-Omega multiple sequence alignment and Needleman-Wunsch global alignment tools on
375 SnapGene. BlastP searches in both NCBI and BV-BRC databases were used to identify
376 homologues of RS05575 in other bacteria. Select homologues were used to generate a multiple
377 sequence alignment for phylogenetic tree using EMBL-EBI's Clustal-Omega. The phylogenetic
378 trees were then modified for readability using the interactive Tree of Life (iTOL) version 6.
379
380 **Protein structure predictions.** Tertiary structures of *E. faecalis* RS05575 and *E. coli* ChuW
381 were obtained using AlphaFold2 Colab notebook and a predictive structure of *E. faecalis*
382 RS05575 binding heme was generated using AlphaFold server. All image files (PDB) were
383 constructed using ChimeraX1.3 (47-49). Structural alignments were performed on the Research
384 Collaboratory for Structural Bioinformatics website using AF-A0A0M2ASD4-F1 (RS05575) and
385 AF_AQFA0A384LP51F1 (ChuW) (31).
386
387 **^{55}Fe uptake.** Overnight cultures of OG1RF were grown in FMC[-Fe]. Cultures were grown to
388 mid-log phase (OD_{600} ~0.5), at which point 1 µM ^{55}Fe (Perkin-Elmer), with and without
389 competing cold metals, was added to each culture followed by incubation at 37°C. Immediately
390 after ^{55}Fe addition and 1 and 5 minutes after, 200 µL aliquots were transferred to a nitrocellulose
391 membrane pre-soaked in 1 M $NiSO_4$ solution (to prevent nonspecific binding) and placed in a

392 slot blot apparatus. Free ^{55}Fe was removed by four washes in 100 mM sodium citrate buffer
393 using vacuum filtration. The membranes were air dried, cut, and dissolved in 4 mL scintillation
394 counter cocktail. Radioactivity was measured by scintillation with “wide open” window setting
395 using a Beckmann LSC6000 scintillation counter. The count per million (cpm) values from ^{55}Fe
396 free cells were obtained and subtracted from the cpm of treated cells. The efficiency of the
397 machine was ~30.8% and was used to convert cpm to disintegrations per minute (dpm), which
398 was then converted to molarity and normalized to CFU.
399
400 **Intracellular heme quantification.** Overnight cultures were grown in FMC[-Fe] under aerobic
401 conditions, and sub-cultures grown under varying degrees of oxygen to OD_{600} 0.4 in FMC +/-
402 iron and/or +/- heme. Specifically, cultures were grown with 50% headspace in a shaking
403 incubator, statically with 50% headspace in an aerobic incubator, statically with no headspace in
404 an aerobic incubator, or statically with no headspace in an anaerobe chamber using media with
405 dissolved oxygen (designated as FMC_{DO} in the text). For heme uptake and degradation kinetic
406 experiments, cultures were first grown in FMC[-Fe] lacking dissolved oxygen (designated as
407 FMC_{O2P}[-Fe]) to OD_{600} 0.4, 10 µM heme was then spiked into the cultures and aliquots taken
408 after 5, 15, and 60 minutes. Degradation of intracellular heme was assessed by growing cells in
409 FMC_{O2P} [-Fe] to OD_{600} 0.4, spiking cultures with 10 µM heme for 15 minutes, and then washing
410 cultures in 0.5mM EDTA in NERL grade metal free PBS once, and in NERL grade metal free
411 PBS twice. The cultures were then resuspended in FMC_{O2P}[-Fe] and samples taken at 0, 60,
412 and 180 minutes after removal of heme. Cells were washed at least 3 times in 1X PBS and
413 lysed using bead beating in 1 mL NERL trace metal grade water. Lysates were used to
414 determine heme content using a heme detection kit (Sigma-Aldrich) and normalized to protein
415 content using the BCA assay (Sigma-Aldrich).
416

Intraperitoneal challenge mouse model. The model has been described previously (43) such that only a brief overview is provided below. To prepare the bacterial inoculum, bacteria were grown in BHI to an OD_{600} of 0.5, the cell pellets collected, washed once in 0.5 mM EDTA and twice in trace metal grade PBS, and suspended in PBS at ~2 x 10^8 CFU mL^{-1}. Seven-week-old C57BL6J mice purchased from Jackson laboratories were intraperitoneally injected with 1 mL of bacterial suspension and euthanized by CO_2 asphyxiation 48-h post-infection. The abdomen was opened to expose the peritoneal lining, 5 mL of cold PBS injected into the peritoneal cavity with 4 mL retrieved as the peritoneal wash content. Quantification of bacteria within the peritoneal cavity was determined by plating serial dilutions on tryptic-soy agar (TSA) containing 200 µg mL^{-1} rifampicin and 10 µg mL^{-1} fusidic acid. For bacterial enumeration inside spleens, livers, kidneys, and hearts, organs were surgically removed, rinsed in 70% ethanol to remove bacteria attached to the exterior of the organ, rinsed in sterile PBS, homogenized in 1 mL PBS, serially diluted, and plated on selective TSA plates. These experiments were approved by the University of Florida Institutional Animal Care and Use Committee (protocol 202200000241).

Infective endocarditis rabbit model. Pathogen-free New Zealand White rabbits (2-4kg; Charles River) were utilized in an endocarditis model as described previously (29). Prior to surgery, rabbits were anesthetized with ketamine, xylazine, glycopyrrolate, buprenorphine, isoflurane, and sevoflurane, with bupivacaine applied locally. A PE-90 catheter (Becton-Dickinson) was inserted into the aortic valve via the right carotid artery; placement was confirmed by ultrasound. Each catheter was tied off and sutured in place, and the incision was closed with staples. Rabbits were monitored for the next 48 hours to ensure stability prior to infection. Bacterial inoculum was prepared by growing cells in BHI. Each strain was washed as described above and normalized to OD_{600} ~0.8 in Chelex-treated (BioRad) PBS. An inoculum was prepared by combining equal volumes of each strain, achieving a total inoculum of 6 x 10^7 CFUs mL^{-1}; 0.5 mL was then delivered via ear vein injection. From the inoculum, 1 mL was

plated and used to verify equal distribution of each strain by PCR using primers listed in Table S3. 24 hours post infection, rabbits were sedated by intramuscular injection with acepromazine (Covetrus) and then euthanized via ear vein injection of Euthasol (Med-Pharmex). Harvested vegetations were placed into PBS, homogenized, and plated on BHI agar. At least 250 colonies per rabbit were analyzed by PCR to determine the percent recovery of each strain that was determined by dividing the number of each specific strain recovered by the total number of colonies assayed and then multiplying by 100. These experiments were approved by the Virginia Commonwealth University Institutional Animal Care and Use Committee (protocol AM10030).

Intestinal colonization mouse model. Seven-week-old C57BL6 male mice were purchased from Jackson Laboratories and given one week to equilibrate their microbiota prior to experimentation. Mice were given antibiotics (0.5 mg/mL cefoperazone + 1 mg/mL vancomycin) in drinking water *ad libitum* for 5 days followed by a 2-day recovery period and subsequent infection. Mice were confirmed culture-negative for endogenous enterococci after vancomycin treatment via selective plating as described below. Mice were infected via oral gavage with 5×10^8 CFUs of *E. faecalis* dissolved in PBS. Enterococcal CFUs were quantified daily from fecal samples. Samples were diluted and homogenized in PBS and serially plated onto bile esculin agar for total enterococci. To distinguish *E. faecalis* lab strains from endogenous enterococci, samples were also grown on bile esculin agar with rifampicin (200 µg/mL). These experiments were approved by the Animal Care and Use Committees of the Children's Hospital of Philadelphia (protocol IAC 21–001316).

Statistical analyses. All data sets were analyzed using GraphPad Prism 10 software. Statistical significance in the transcriptional expression studies were analyzed by comparing the fold change in copy number before and after heme supplementation using a Student's T-test.

Statistical differences in ^{55}Fe uptake were determined by Two-way ANOVA and Dunnett's multiple comparison test. Intracellular heme content of OG1RF grown in the presence or absence of oxygen, with or without an excess iron source was analyzed by Student's T-test. The intracellular heme content of strains grown in decreasing oxygen levels was analyzed with a Two-way ANOVA and Šidák's multiple comparison test. Statistical significance in the mouse peritonitis and in the gut colonization model were determined by the Mann Whitney test. Statistical differences in recovery of strains from the competitive rabbit IE model was determined by a repeated measure One-way ANOVA with a pairwise Holm Šidák's multiple comparison test.

ACKNOWLEDGEMENTS. We thank Drs. Jennifer Bradley, Liang Bao, and Josephina Vossen and Ms. Kali Williams, Katherine Atran, Valerie Assi and Nicai Zollar for assistance with the rabbit endocarditis model. This study was supported by NIH-NIAID grant R21 AI137446 to J.A.L and R35GM138369 to J.P.Z. D.N.B. was supported by NIH-NIDCR training grant T90 DE021990 and by American Heart Association predoctoral fellowship 907592. J.P.Z. was also supported by the Center for Microbial Medicine at the Children's Hospital of Philadelphia.

Table 1. Bacterial strains used in this study.

Strains	Relevant Characteristics	Source
E. faecalis		
OG1RF	Rif^R Fus^R	Lab collection
Δ*efaCBA*Δ*feoB*Δ*fhuB*Δ*fitAB*Δ*emtB* (Δ5Fe)	*efaCBA* deletion; *feoB* deletion; *fhuB* deletion; *fitAB* deletion; *emtB* deletion.	(9)
ΔRS05575	RS05575 deletion.	This study
ΔRS05575c	RS05575 complemented with reintegration.	This study
Δ5FeΔRS05575	RS05575 deletion; *efaCBA* deletion; *feoB* deletion; *fhuB* deletion; *fitAB* deletion; *emtB* deletion.	This study
Δ5FeΔRS05575c	RS05575 deletion; *efaCBA* deletion; *feoB* deletion; *fhuB* deletion; *fitAB* deletion; *emtB* deletion. RS05575 complemented with reintegration.	This study
CK111	OG1S *upp4::*P23*repA4,* $Spec^R$. Conjugation donor strain.	(46)

FIGURE LEGENDS

Fig 1. *Enterococcus faecalis* uses heme as an iron source. (**A**) ^{55}Fe uptake by *E. faecalis* is diminished by competition with unlabeled heme and iron. OG1RF was grown in FMC[-Fe] to OD_{600} 0.5 and ^{55}Fe uptake monitored at one and five minutes after addition of 1µM ^{55}Fe, 1µM ^{55}Fe + 10µM heme, or 1µM ^{55}Fe + 40µM $FeSO_4$. Statistical significance was determined by Two-Way ANOVA with Dunnett's multiple comparison test. (**B**) RT-PCR analysis showing that heme supplementation represses iron uptake genes but activates transcription of manganese uptake genes. OG1RF was grown to OD_{600} 0.5 in FMC[-Fe] and sampled before and 60 minutes after supplementation with 20 µM heme. Statistical significance was determined by Student's T-test. (**C**) Excess iron leads to increased intracellular heme levels. OG1RF was grown in either FMC[-Fe +20 µM heme] or FMC[+10 µM Fe +20 µM heme] to OD_{600} 0.5 and the intracellular heme content determined. Statistical significance was determined by a Student's T-test, *p≤0.05, **p≤0.01, ****p≤0.0001.

Fig 2. Identification of a putative anaerobilin synthase in *E. faecalis*. (**A**) Amino acid alignment of *E. faecalis* RS05575 and *E. coli* ChuW. The canonical rSAM CXXXCXXC motif is outlined in red, the aspartic acid residue known to be important for ChuW activity is outlined in green, and residues conserved across *E. coli* ChuW, *Vibrio cholerae* HutW, and *Fusobacterium nucleatum* HmuW are outlined in blue. (**B**) AlphaFold 2 structures of *E. faecalis* RS05575 and *E. coli* ChuW superimposed on each other using ChimeraX.

Fig 3. Phylogenetic analysis of RS05575 homologues in other Gram-positive facultative anaerobes and select Gram-negatives. BlastP searches against RS05575 were used to identify homologues across species of enterococci, streptococci, staphylococci, *E. coli*, *V. cholerae*, and *F. nucleatum*. Phylogenetic trees were constructed using multiple sequence alignments of representative species using Clustal Omega and iTOL.

Fig 4. Growth of *E. faecalis* OG1RF and ΔRS05575 strains in media containing different amounts of $FeSO_4$ and heme and under different atmospheres. (**A**) FMC[-Fe], (**B**) FMC[+20 µM Fe], (**C**) FMC[+20 µM heme], (**D**) FMC_{DO}[-Fe], (**E**) FMC_{DO}[+20 µM Fe], (**F**) FMC_{DO}[+20 µM heme], (**G**) FMC_{O2P}[-Fe], (**H**) FMC_{O2P}[+20 µM Fe], and (**I**) FMC_{O2P}[+20 µM heme]. Cells were grown overnight in FMC[-Fe], FMC_{DO}[-Fe], or FMC_{O2P}[-Fe], normalized to OD_{600} 0.2 and sub-cultured at 1:200 into the designated media. Growth was monitored by measuring OD_{600} every 30 minutes using an automated growth reader. The ΔRS05575c strain was used to show genetic complementation of the more noticeable phenotypes (**C**, **G** and **I**). Error bars denote standard error of the mean from at least two independent experiments with three biological replicates each.

Fig 5. RS05575 degrades heme under oxygen-depleted conditions. (**A**) Strains were grown in FMC[+20 µM heme] to OD_{600} ~0.5 in a shaking incubator with 50% headspace, a static incubator with 50% headspace, a static incubator with no headspace, or in the anaerobic chamber with no headspace. All media contained dissolved oxygen to bypass the extreme growth defect under anaerobic conditions in the presence of heme. (**B, C**) Intracellular heme content of OG1RF, ΔRS05575, and ΔRS05575c. Individual biological replicates from at least 2 independent experiments shown with n≥8. Error bars denote standard error of the mean. Statistical significance was determined by a Two-way ANOVA with Šidák's multiple comparison test,*p≤0.05, **p≤0.01, ***p≤0.001 ****p≤0.0001.

Fig 6. Uptake and degradation of heme by RS05575 in anaerobic conditions. (**A**) OG1RF, ΔRS05575, Δ5Fe, and Δ5FeΔRS05575 were grown to OD_{600} ~0.5 in FMC_{O2P}[-Fe] at which point cultures were supplemented with 10 µM heme and the intracellular heme determined after 0, 5, 15, and 60 minutes. (**B**) Cultures were supplemented with 10 µM heme for 15 minutes, washed, and cell pellets suspended in FMC_{O2P}[-Fe]. Samples were taken at 0, 60, and 180 minutes after

heme removal. All data was normalized to protein content. Experiments were performed with 3 biological replicates on at least two independent occasions. Error bars denote standard error of the mean. Statistical significance was determined by an ordinary One-way ANOVA with Dunnett's multiple comparisons test at each time point,*p≤0.05, **p≤0.01, ***p≤0.001 ****p≤0.0001.

Fig 7. Loss of RS05575 and all 5 iron transporters (Δ5Fe strain) alone or in combination differentially affects *E. faecalis* virulence potential. 7-week-old C57BL6-J mice from Jackson Laboratories were infected with $1X10^8$ CFUs via intraperitoneal injection and the mice euthanizes after 48 hours and the different tissues collected for CFU determination. (**A**) peritoneal wash, (**B**) spleens, (**C**) hearts, (**D**) livers, and (**E**) kidneys. The data points shown are a result of the ROUT outlier test and bars denote median values. Statistical analyses were performed using the Mann-Whitney test, *p≤0.05, **p≤0.01, ***p p≤0.001, and ****p≤0.0001.

Fig 8. Competitive fitness of OG1RF, ΔRS05575, Δ5Fe, and Δ5FeΔRS05575 in a rabbit infective endocarditis model. Bacteria was co-inoculated (1:1:1:1 ratio) into the ear vein of rabbits 48-hours after catheter implantation. After 24-hours animals were euthanized and bacterial burdens determined in the heart vegetations. (**A**) Schematic of model. (**B**) Graph shows the percent of each strain recovered from each animal. Each symbol represents an individual rabbit, and the horizontal line represents the median recovery of each strain. Statistical significance was determined using a repeated measures one-way ANOVA with a Holm-Šidák's multiple comparisons test, ** p≤0.01.

Fig 9. Competitive fitness of OG1RF, ΔRS05575, Δ5Fe, and Δ5FeΔRS05575 in a mouse gut colonization model. Seven-week-old C57BL6J mice were given vancomycin in drinking water to deplete endogenous enterococci prior to inoculation with *E. faecalis* strains by oral gavage.

567 Feces were collected every day for 3 days for CFU determination. (**A**) Schematic of gut
568 colonization model. (**B**) Colonization of mice by OG1RF, ΔRS05575, Δ5Fe, or Δ5FeΔRS05575
569 was determined by plating stool samples on bile esculin agar with rifampicin (200 μg mL^{-1}). Data
570 are shown with median. Statistical significance was determined by multiple Mann-Whitney tests
571 for significance with Bonferroni-Dunn correction for multiple comparisons, *p≤0.05, **p≤0.01,
572 ***p p≤0.001, and ****p≤0.0001.
573

REFERENCES

1. García-Solache M, Rice LB. 2019. The Enterococcus: a Model of Adaptability to Its Environment. Clin Microbiol Rev 32.
2. Ramsey M, Hartke A, Huycke M. 2014. The Physiology and Metabolism of Enterococci. *In* Gilmore MS, Clewell DB, Ike Y, Shankar N (ed), Enterococci: From Commensals to Leading Causes of Drug Resistant Infection, Boston.
3. Gaca AO, Lemos JA. 2019. Adaptation to Adversity: the Intermingling of Stress Tolerance and Pathogenesis in Enterococci. *Microbiol Mol Biol Rev* 83.
4. Skaar1 TEK-FaEP. 2010. Nutritional immunity beyond iron: a role for manganese and zinc. NIH-PA Current Opinions in Chemical Biology.
5. Murdoch CC, Skaar EP. 2022. Nutritional immunity: the battle for nutrient metals at the host-pathogen interface. Nat Rev Microbiol doi:10.1038/s41579-022-00745-6.
6. Diaz-Ochoa VE, Jellbauer S, Klaus S, Raffatellu M. 2014. Transition metal ions at the crossroads of mucosal immunity and microbial pathogenesis. Front Cell Infect Microbiol 4:2.
7. Palmer LD, Skaar EP. 2016. Transition Metals and Virulence in Bacteria. *Annu Rev Genet* 50:67-91.
8. Cassat JE, Skaar EP. 2013. Iron in infection and immunity. *Cell Host Microbe* 13:509-519.
9. Brunson DN, Colomer-Winter C, Lam LN, Lemos JA. 2023. Identification of Multiple Iron Uptake Mechanisms in Enterococcus faecalis and Their Relationship to Virulence. Infect Immun 91:e0049622.
10. Ratledge C, Dover LG. 2000. Iron metabolism in pathogenic bacteria. *Annual Review of Microbiology* 54:881-941.
11. Nobles CL, Maresso AW. 2011. The theft of host heme by Gram-positive pathogenic bacteria. Metallomics 3:788-96.
12. Runyen-Janecky LJ. 2013. Role and regulation of heme iron acquisition in gram-negative pathogens. Front Cell Infect Microbiol 3:55.
13. Choby JE, Skaar EP. 2016. Heme Synthesis and Acquisition in Bacterial Pathogens. *J Mol Biol* 428:3408-28.
14. Coates CJ, Nairn J. 2014. Diverse immune functions of hemocyanins. *Dev Comp Immunol* 45:43-55.
15. Frankenberg L, Brugna M, Hederstedt L. 2002. *Enterococcus faecalis* Heme-Dependent Catalase. *Journal of Bacteriology* 184:6351-6356.
16. Winstedt L, Frankenberg L, Hederstedt L, von Wachenfeldt C. 2000. *Enterococcus faecalis* V583 contains a cytochrome bd-type respiratory oxidase. *J Bacteriol* 182:3863-6.
17. Lyles KV, Eichenbaum Z. 2018. From Host Heme To Iron: The Expanding Spectrum of Heme Degrading Enzymes Used by Pathogenic Bacteria. Front Cell Infect Microbiol 8:198.
18. Li C, Stocker R. 2009. Heme oxygenase and iron: from bacteria to humans. Redox Rep 14:95-101.
19. Skaar EP, Gaspar AH, Schneewind O. 2006. Bacillus anthracis IsdG, a heme-degrading monooxygenase. J Bacteriol 188:1071-80.
20. Reniere ML, Ukpabi GN, Harry SR, Stec DF, Krull R, Wright DW, Bachmann BO, Murphy ME, Skaar EP. 2010. The IsdG-family of haem oxygenases degrades haem to a novel chromophore. Mol Microbiol 75:1529-38.
21. Reniere ML, Skaar EP. 2008. Staphylococcus aureus haem oxygenases are differentially regulated by iron and haem. Mol Microbiol 69:1304-15.
22. LaMattina JW, Nix DB, Lanzilotta WN. 2016. Radical new paradigm for heme degradation in Escherichia coli O157:H7. Proc Natl Acad Sci U S A 113:12138-12143.

23. Mathew LG, Beattie NR, Pritchett C, Lanzilotta WN. 2019. New Insight into the Mechanism of Anaerobic Heme Degradation. Biochemistry 58:4641-4654.
24. Brimberry M, Toma MA, Hines KM, Lanzilotta WN. 2021. HutW from Vibrio cholerae Is an Anaerobic Heme-Degrading Enzyme with Unique Functional Properties. Biochemistry 60:699-710.
25. McGregor AK, Chan ACK, Schroeder MD, Do LTM, Saini G, Murphy MEP, Wolthers KR. 2023. A new member of the flavodoxin-superfamily from Fusobacterium nucleatum that functions in heme-trafficking and reduction of anaerobilin. J Biol Chem doi:10.1016/j.jbc.2023.104902:104902.
26. Brunson DN, Lemos JA. 2024. Heme utilization by the enterococci. FEMS Microbes 5:xtae019.
27. Ch'ng JH, Muthu M, Chong KKL, Wong JJ, Tan CAZ, Koh ZJS, Lopez D, Matysik A, Nair ZJ, Barkham T, Wang Y, Kline KA. 2022. Heme cross-feeding can augment *Staphylococcus aureus* and *Enterococcus faecalis* dual species biofilms. *ISME J* 16:2015-2026.
28. Terleckyj B, Willett NP, Shockman GD. 1975. Growth of several cariogenic strains of oral streptococci in a chemically defined medium. *Infect Immun* 11:649-55.
29. Colomer-Winter C, Flores-Mireles AL, Baker SP, Frank KL, Lynch AJL, Hultgren SJ, Kitten T, Lemos JA. 2018. Manganese acquisition is essential for virulence of *Enterococcus faecalis*. *PLoS Pathog* 14:e1007102.
30. Saillant V, Lipuma D, Ostyn E, Joubert L, Boussac A, Guerin H, Brandelet G, Arnoux P, Lechardeur D. 2021. A Novel *Enterococcus faecalis* Heme Transport Regulator (FhtR) Senses Host Heme To Control Its Intracellular Homeostasis. *mBio* 12.
31. Bittrich S, Segura J, Duarte JM, Burley SK, Rose Y. 2024. RCSB protein Data Bank: exploring protein 3D similarities via comprehensive structural alignments. Bioinformatics 40.
32. Smith AB, Jenior ML, Keenan O, Hart JL, Specker J, Abbas A, Rangel PC, Di C, Green J, Bustin KA, Gaddy JA, Nicholson MR, Laut C, Kelly BJ, Matthews ML, Evans DR, Van Tyne D, Furth EE, Papin JA, Bushman FD, Erlichman J, Baldassano RN, Silverman MA, Dunny GM, Prentice BM, Skaar EP, Zackular JP. 2022. Enterococci enhance Clostridioides difficile pathogenesis. Nature 611:780-786.
33. Smith AB, Specker JT, Hewlett KK, Scoggins TRt, Knight M, Lustig AM, Li Y, Evans KM, Guo Y, She Q, Christopher MW, Garrett TJ, Moustafa AM, Van Tyne D, Prentice BM, Zackular JP. 2024. Liberation of host heme by Clostridioides difficile-mediated damage enhances Enterococcus faecalis fitness during infection. mBio 15:e0165623.
34. Wang M, Wang Y, Wang M, Liu M, Cheng A. 2023. Heme acquisition and tolerance in Gram-positive model bacteria: An orchestrated balance. Heliyon 9:e18233.
35. Layer G. 2021. Heme biosynthesis in prokaryotes. Biochim Biophys Acta Mol Cell Res 1868:118861.
36. Frankenberg-Dinkel N. 2004. Bacterial heme oxygenases. Antioxid Redox Signal 6:825-34.
37. Womack E, Alibayov B, Vidal JE, Eichenbaum Z. 2024. Endogenously produced H(2)O(2) is intimately involved in iron metabolism in Streptococcus pneumoniae. Microbiol Spectr 12:e0329723.
38. McDevitt E, Khan F, Scasny A, Thompson CD, Eichenbaum Z, McDaniel LS, Vidal JE. 2020. Hydrogen Peroxide Production by Streptococcus pneumoniae Results in Alpha-hemolysis by Oxidation of Oxy-hemoglobin to Met-hemoglobin. mSphere 5.
39. Alibayov B, Scasny A, Khan F, Creel A, Smith P, Vidal AGJ, Fitisemanu FM, Padilla-Benavides T, Weiser JN, Vidal JE. 2022. Oxidative Reactions Catalyzed by Hydrogen Peroxide Produced by Streptococcus pneumoniae and Other Streptococci Cause the Release and Degradation of Heme from Hemoglobin. Infect Immun 90:e0047122.

40. La Carbona S, Sauvageot N, Giard JC, Benachour A, Posteraro B, Auffray Y, Sanguinetti M, Hartke A. 2007. Comparative study of the physiological roles of three peroxidases (NADH peroxidase, Alkyl hydroperoxide reductase and Thiol peroxidase) in oxidative stress response, survival inside macrophages and virulence of Enterococcus faecalis. Mol Microbiol 66:1148-63.
41. Colomer-Winter C, Gaca AO, Lemos JA. 2017. Association of Metal Homeostasis and (p)ppGpp Regulation in the Pathophysiology of *Enterococcus faecalis*. *Infect Immun* 85.
42. Choby JE, Skaar EP. 2019. Staphylococcus aureus Coproporphyrinogen III Oxidase Is Required for Aerobic and Anaerobic Heme Synthesis. mSphere 4.
43. Grunenwald A, Roumenina LT, Frimat M. 2021. Heme Oxygenase 1: A Defensive Mediator in Kidney Diseases. Int J Mol Sci 22.
44. Khalili H, de Silva PS, Ananthakrishnan AN, Lochhead P, Joshi A, Garber JJ, Richter JR, Sauk J, Chan AT. 2017. Dietary Iron and Heme Iron Consumption, Genetic Susceptibility, and Risk of Crohn's Disease and Ulcerative Colitis. Inflamm Bowel Dis 23:1088-1095.
45. Lopez CA, Skaar EP. 2018. The Impact of Dietary Transition Metals on Host-Bacterial Interactions. *Cell Host Microbe* 23:737-748.
46. Kristich CJ, Manias DA, Dunny GM. 2005. Development of a method for markerless genetic exchange in *Enterococcus faecalis* and its use in construction of a *srtA* mutant. *Appl Environ Microbiol* 71:5837-49.
47. Pettersen EF, Goddard TD, Huang CC, Couch GS, Greenblatt DM, Meng EC, Ferrin TE. 2004. UCSF Chimera--a visualization system for exploratory research and analysis. J Comput Chem 25:1605-12.
48. Varadi M, Anyango S, Deshpande M, Nair S, Natassia C, Yordanova G, Yuan D, Stroe O, Wood G, Laydon A, Zidek A, Green T, Tunyasuvunakool K, Petersen S, Jumper J, Clancy E, Green R, Vora A, Lutfi M, Figurnov M, Cowie A, Hobbs N, Kohli P, Kleywegt G, Birney E, Hassabis D, Velankar S. 2022. AlphaFold Protein Structure Database: massively expanding the structural coverage of protein-sequence space with high-accuracy models. Nucleic Acids Res 50:D439-D444.
49. Jumper J, Evans R, Pritzel A, Green T, Figurnov M, Ronneberger O, Tunyasuvunakool K, Bates R, Zidek A, Potapenko A, Bridgland A, Meyer C, Kohl SAA, Ballard AJ, Cowie A, Romera-Paredes B, Nikolov S, Jain R, Adler J, Back T, Petersen S, Reiman D, Clancy E, Zielinski M, Steinegger M, Pacholska M, Berghammer T, Bodenstein S, Silver D, Vinyals O, Senior AW, Kavukcuoglu K, Kohli P, Hassabis D. 2021. Highly accurate protein structure prediction with AlphaFold. Nature 596:583-589.

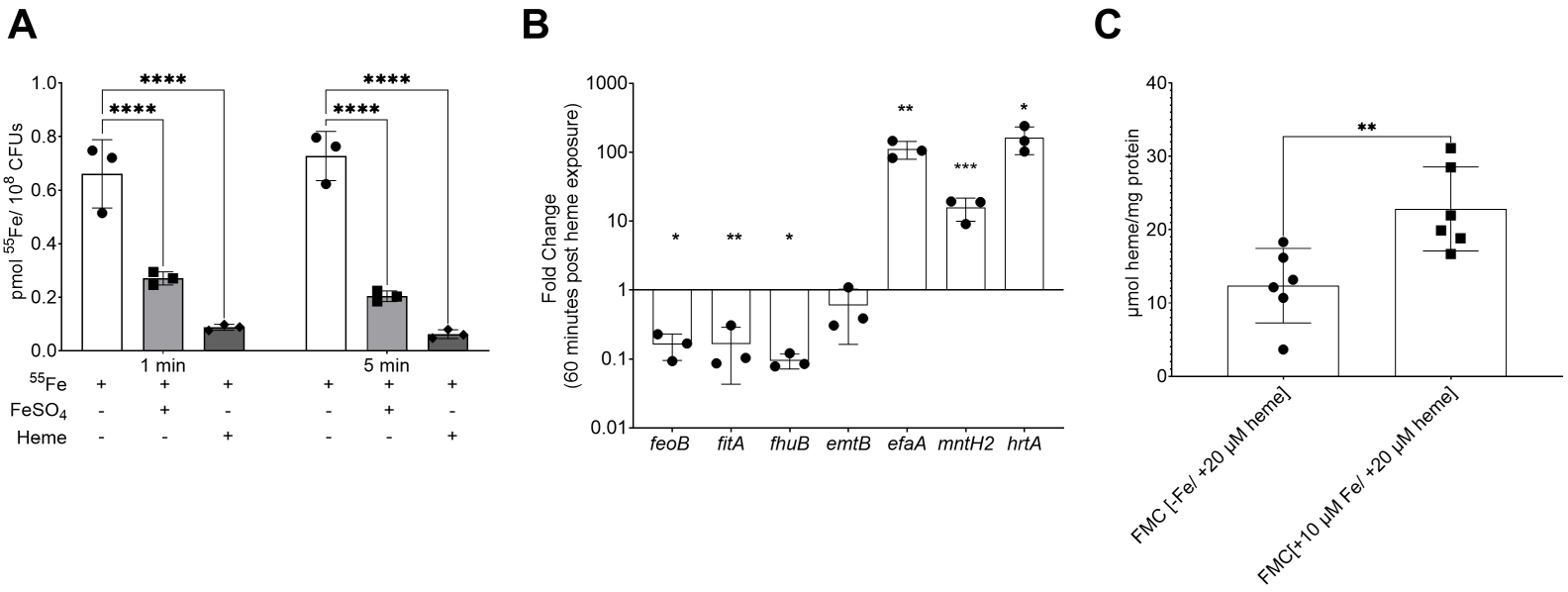

A

```
E. coli ChuW      58  RLVYLHIPFCATHCTFCGFYQNRFNEDACAHYTDALIREIEMEADSVLHQSAPIHAVYFGGGSPSALSAHDLARI  132
                      R  Y+HIPFC   C +C F +          Y  +L++EI++     L+    +  +Y GGG+P++LSA  L  +
E. faecalis RS05575  4  RSAYIHIPFCEHICYYCDFNKVFLEGQPVDEYIQSLLKEIQL--TQALYPEQEMKTIYIGGGTPTSLSAKQLDVL   76

E. coli ChuW      133 ITTLREKLPLAPDCEITIEGRVLNFDAERIDACLDAGANRFSIGIQSFNSKIRKKMARTSDGPTAIAFMESLVKR  207
                      +  +R++L      E T+E    +   E++    + G NR S+G+Q+F+ ++ KK+ R          M+ L K
E. faecalis RS05575  77  LKGVRKQLTFDDRNEFTVEANPGDLTQEKLQVMKNYGVNRLSMGVQTFDDRLLKKIGRKHTAADVYETMKFLEKE  151

E. coli ChuW      208 DRAAVVCDLLFGLPGQDAQTWGEDLAIARDIGLDGVDLYALNVLSNTPLGKAVENGRTTVPSPAERRDLYLQGCD  282
                      +   V  DL++ LPGQ  +++ + L  A  + L   LY+L + + T     V  GR  +P       ++ +  +
E. faecalis RS05575  152 NFTNVSIDLIYALPGQTLESFRDTLTRALALDLPHYSLYSLILENKTMFMNWVRQGRLQLPEEEIEAQMFDETIE  226

E. coli ChuW      283 FMDDAGWRCISNSHWGRTTRERNLYNLLIKQGADCLAFGSGAGGSINGYSWMNERNLQTWHESVAAGKKPL----  353
                       M+  G      S++  T +E + +NL         FG+GA G +    + N   +Q + + +    + P+
E. faecalis RS05575  227 AMEKKGRHQYEVSNFALTGKE-SQHNLAYWNNDHYYGFGAGASGYLGQTRYKNHGPIQHYLKPLRENQLPIVETE  300

E. coli ChuW      353 -MLIMRNAERNAQWRHTLQSGVETARVPLDELTPHAEKLAPLLAQWHQKGLSRDASTCLRLTNEGRFWASNILQS  427
                       +  +   E        + G+   +       P       ++ +  ++ L  + +  LRLT +G F  +N+ ++
E. faecalis RS05575  301 ELTRLNQIEEELFLGLRKKVGISKQKFQQKFQEPIEAIYGEVIQRLIKEELLIEEADILRLTKKGLFVGNNVFEA  375
```

B

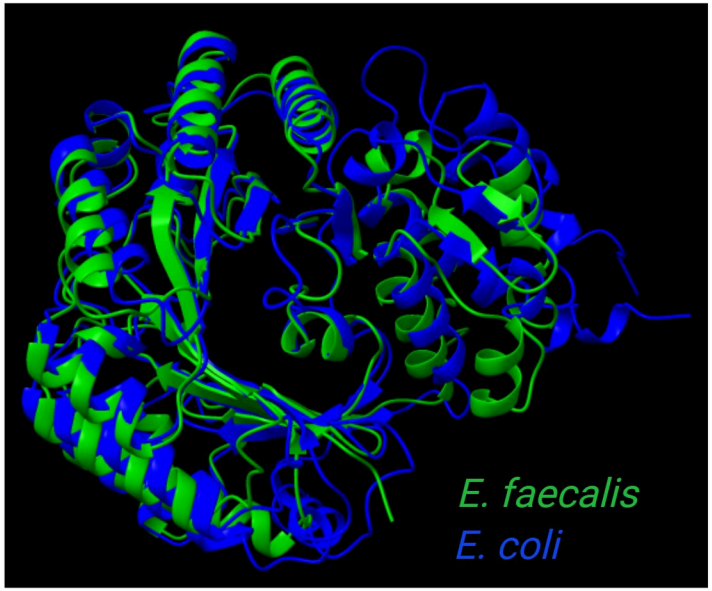

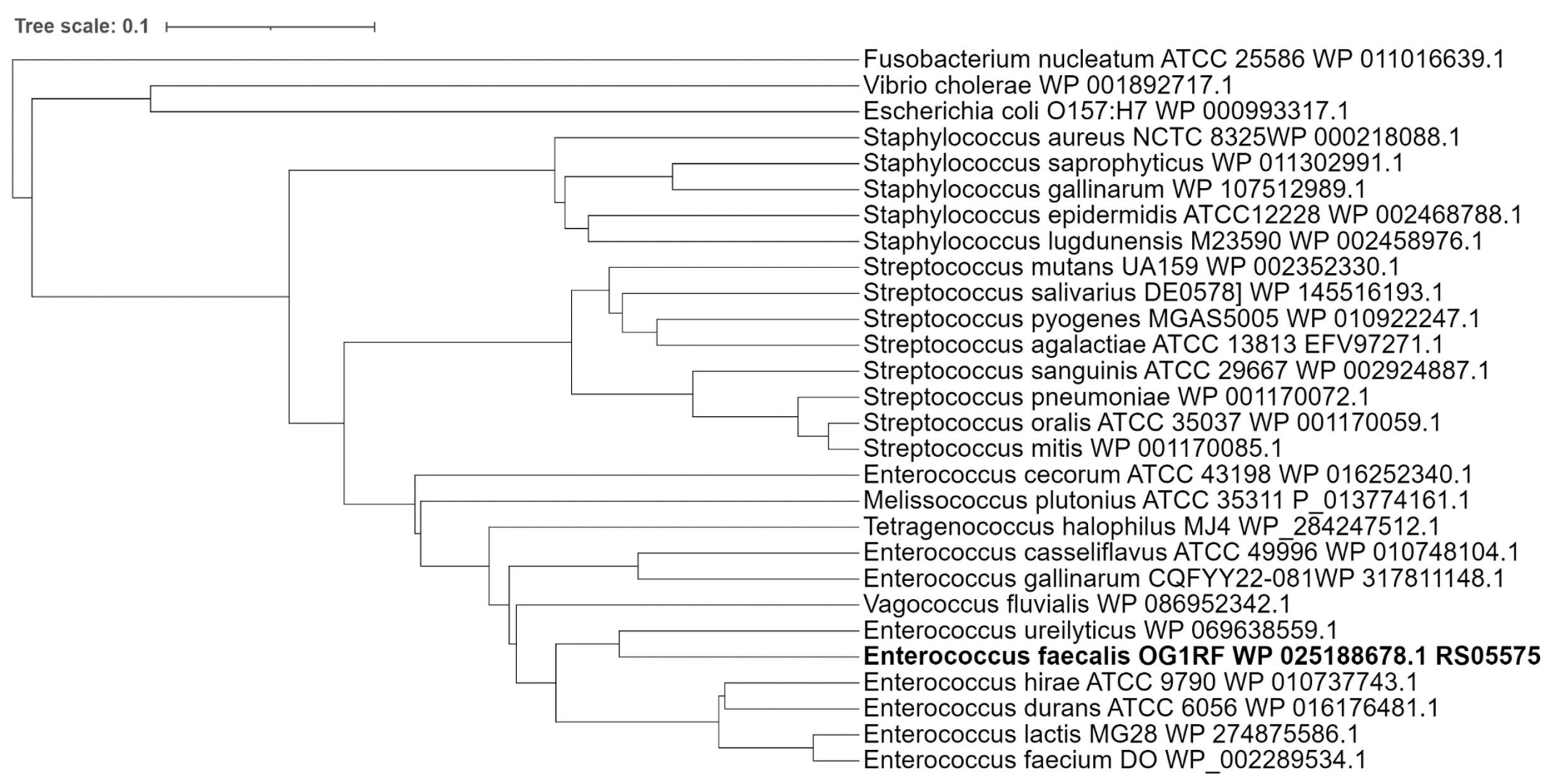
Tree scale: 0.1
Fusobacterium nucleatum ATCC 25586 WP 011016639.1
Vibrio cholerae WP 001892717.1
Escherichia coli O157:H7 WP 000993317.1
Staphylococcus aureus NCTC 8325WP 000218088.1
Staphylococcus saprophyticus WP 011302991.1
Staphylococcus gallinarum WP 107512989.1
Staphylococcus epidermidis ATCC12228 WP 002468788.1
Staphylococcus lugdunensis M23590 WP 002458976.1
Streptococcus mutans UA159 WP 002352330.1
Streptococcus salivarius DE0578] WP 145516193.1
Streptococcus pyogenes MGAS5005 WP 010922247.1
Streptococcus agalactiae ATCC 13813 EFV97271.1
Streptococcus sanguinis ATCC 29667 WP 002924887.1
Streptococcus pneumoniae WP 001170072.1
Streptococcus oralis ATCC 35037 WP 001170059.1
Streptococcus mitis WP 001170085.1
Enterococcus cecorum ATCC 43198 WP 016252340.1
Melissococcus plutonius ATCC 35311 P_013774161.1
Tetragenococcus halophilus MJ4 WP_284247512.1
Enterococcus casseliflavus ATCC 49996 WP 010748104.1
Enterococcus gallinarum CQFYY22-081WP 317811148.1
Vagococcus fluvialis WP 086952342.1
Enterococcus ureilyticus WP 069638559.1
Enterococcus faecalis OG1RF WP 025188678.1 RS05575
Enterococcus hirae ATCC 9790 WP 010737743.1
Enterococcus durans ATCC 6056 WP 016176481.1
Enterococcus lactis MG28 WP 274875586.1
Enterococcus faecium DO WP_002289534.1

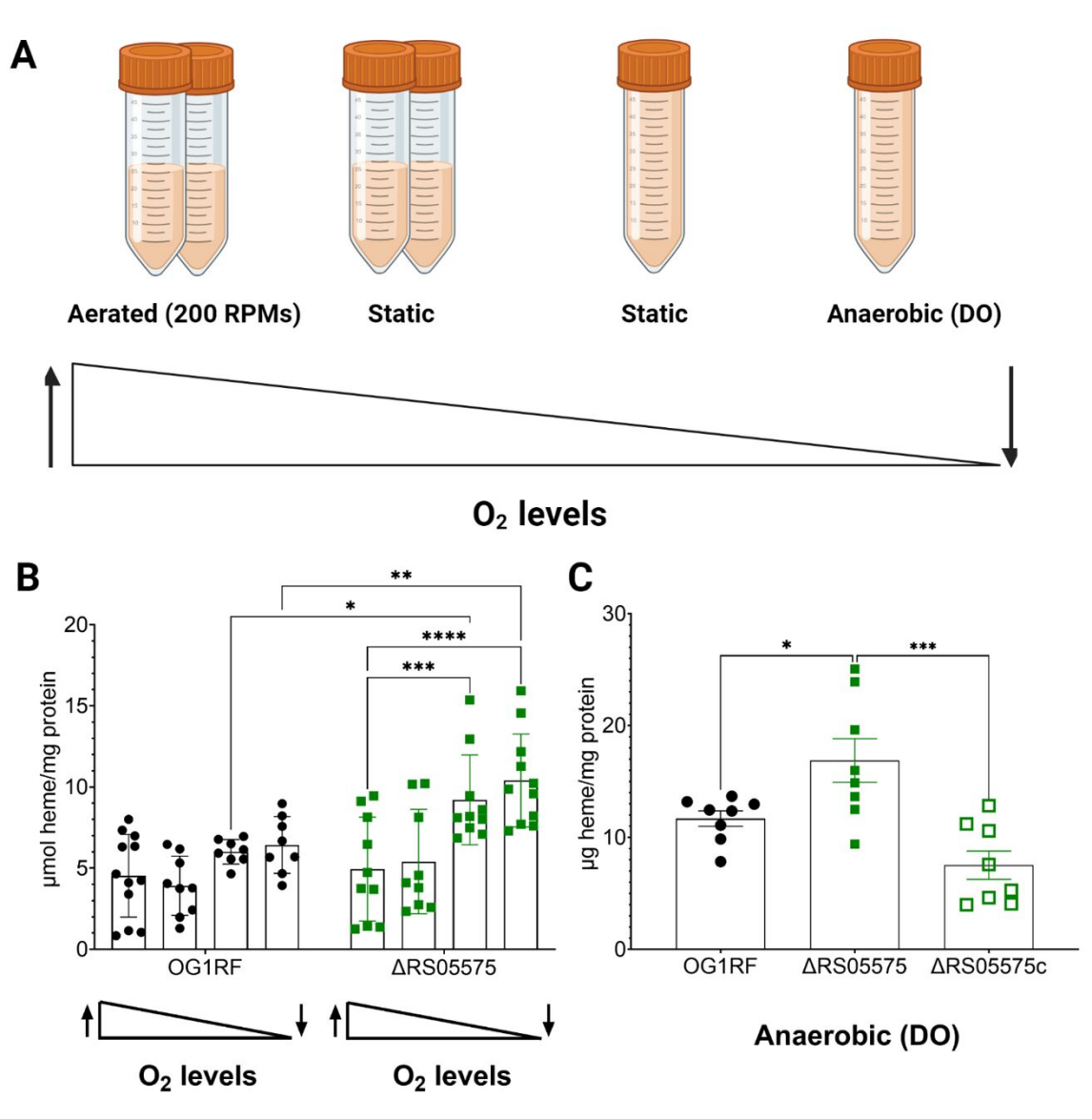
A
Aerated (200 RPMs)
Static
Static
Anaerobic (DO)
O2 levels
B
µmol heme/mg protein
20
15
10
5
0
**
*
****
***
OG1RF
ΔRS05575
O2 levels
O2 levels
C
µg heme/mg protein
30
20
10
0
*
***
OG1RF
ΔRS05575
ΔRS05575c
Anaerobic (DO)

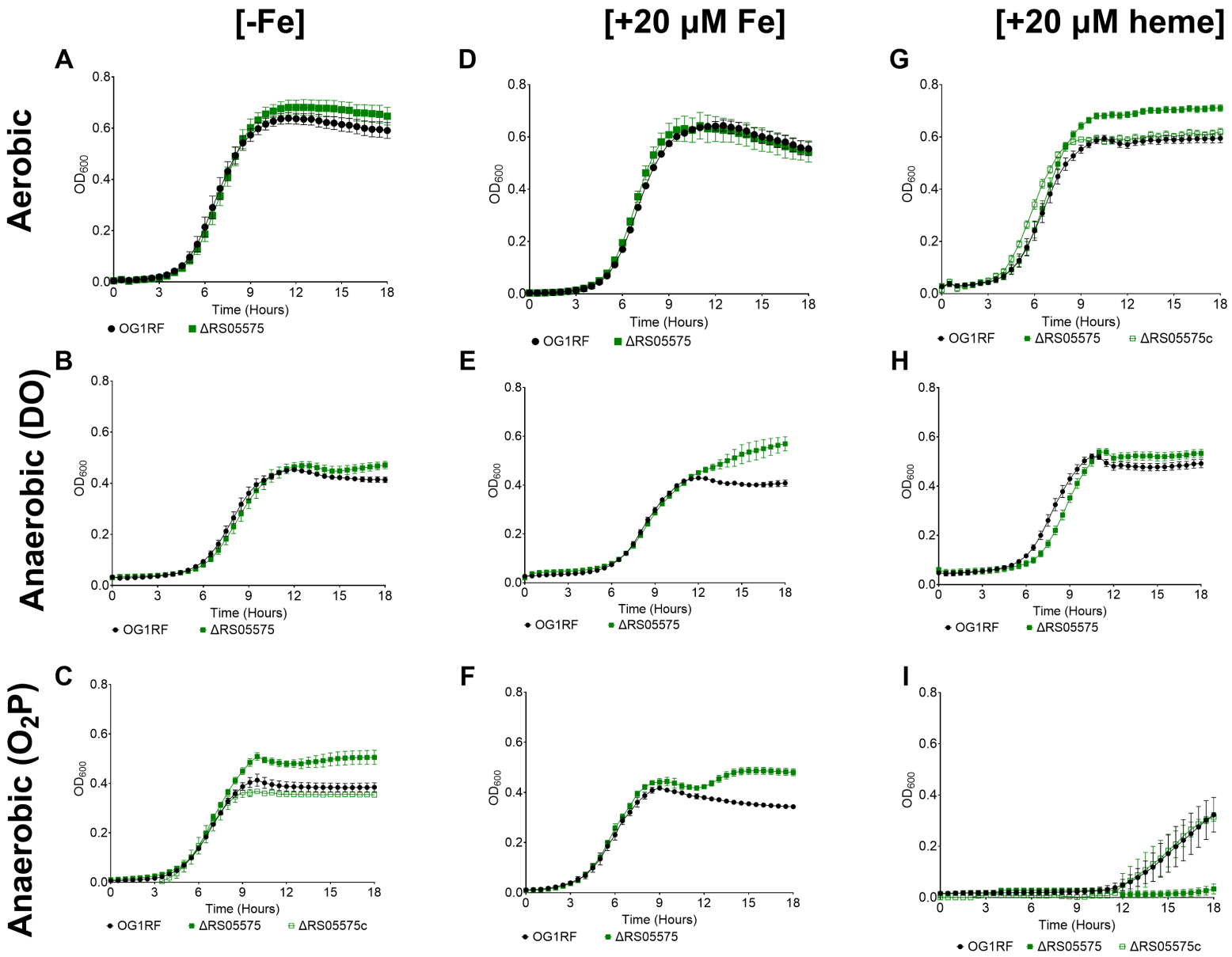

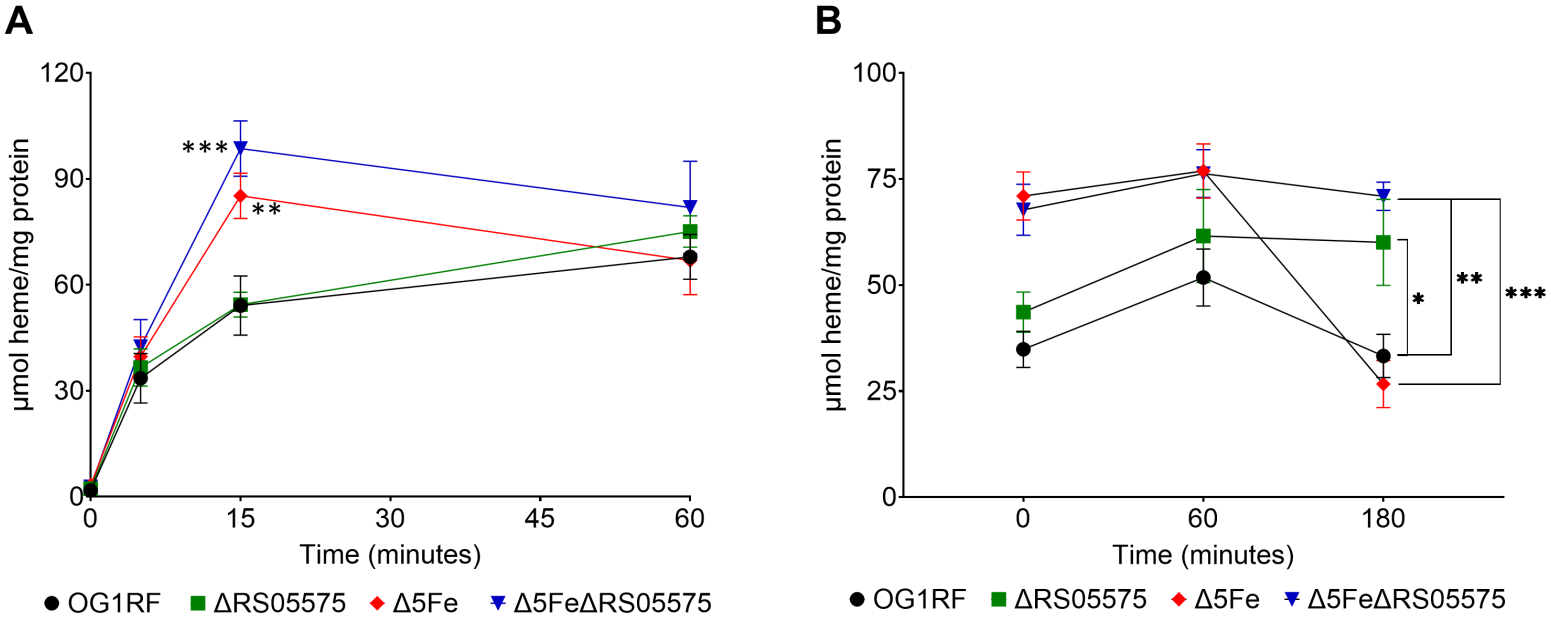

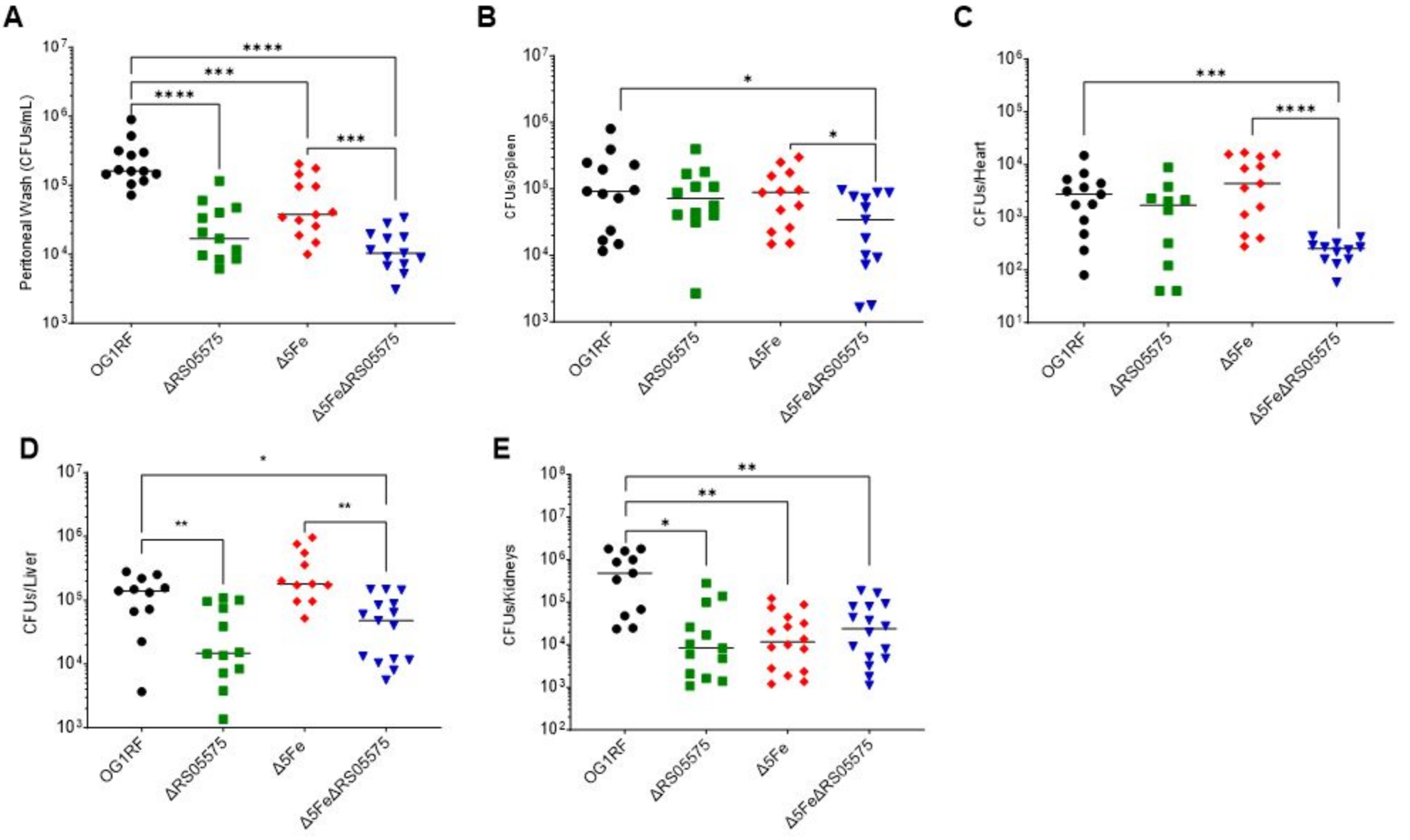
A
Peritoneal Wash (CFUs/mL)
10^7
10^6
10^5
10^4
10^3
****
***
****
***
OG1RF
ΔRS05575
Δ5Fe
Δ5FeΔRS05575
B
CFUs/Spleen
10^7
10^6
10^5
10^4
10^3
*
*
OG1RF
ΔRS05575
Δ5Fe
Δ5FeΔRS05575
C
CFUs/Heart
10^6
10^5
10^4
10^3
10^2
10^1
***
****
OG1RF
ΔRS05575
Δ5Fe
Δ5FeΔRS05575
D
CFUs/Liver
10^7
10^6
10^5
10^4
10^3
*
**
**
OG1RF
ΔRS05575
Δ5Fe
Δ5FeΔRS05575
E
CFUs/Kidneys
10^8
10^7
10^6
10^5
10^4
10^3
10^2
**
**
*
OG1RF
ΔRS05575
Δ5Fe
Δ5FeΔRS05575

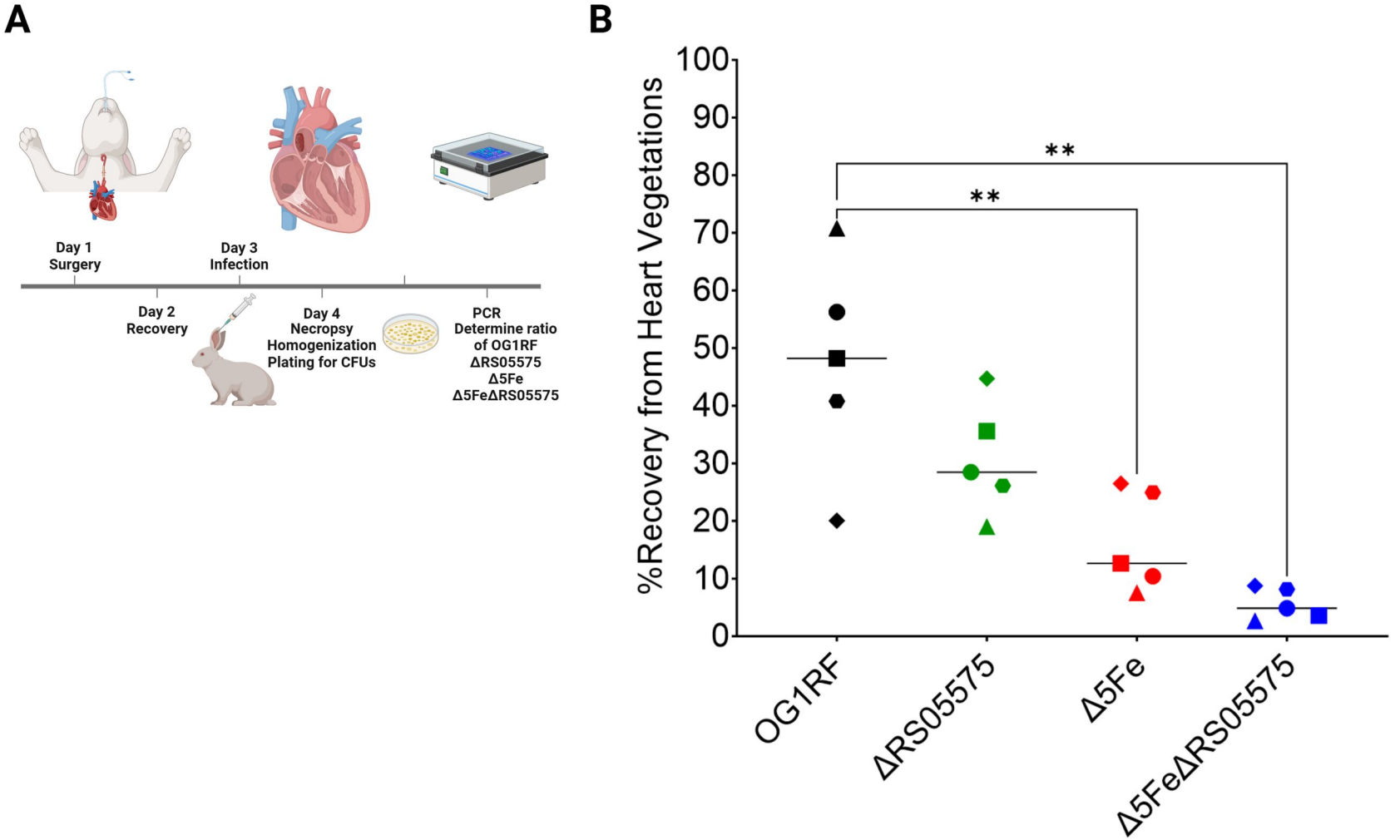
A
Day 1
Surgery
Day 3
Infection
Day 2
Recovery
Day 4
Necropsy
Homogenization
Plating for CFUs
PCR
Determine ratio
of OG1RF
ΔRS05575
Δ5Fe
Δ5FeΔRS05575
B
%Recovery from Heart Vegetations
100
90
80
70
60
50
40
30
20
10
0
**
**
OG1RF
ΔRS05575
Δ5Fe
Δ5FeΔRS05575

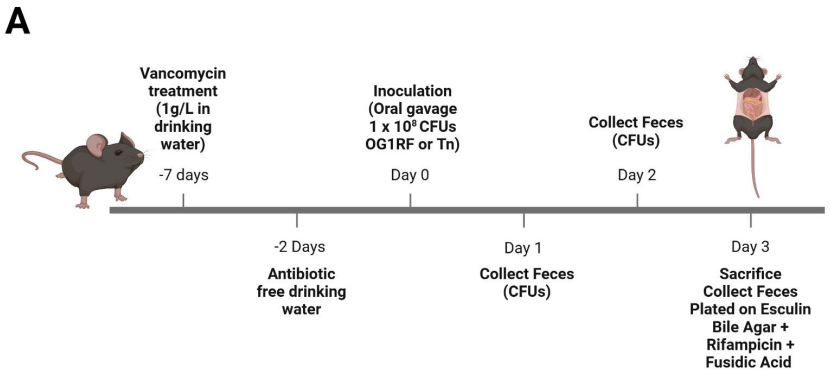
A
Vancomycin treatment (1g/L in drinking water)
-7 days
Inoculation (Oral gavage 1 x 10⁸ CFUs OG1RF or Tn)
Day 0
Collect Feces (CFUs)
Day 2
-2 Days
Antibiotic free drinking water
Day 1
Collect Feces (CFUs)
Day 3
Sacrifice Collect Feces Plated on Esculin Bile Agar + Rifampicin + Fusidic Acid

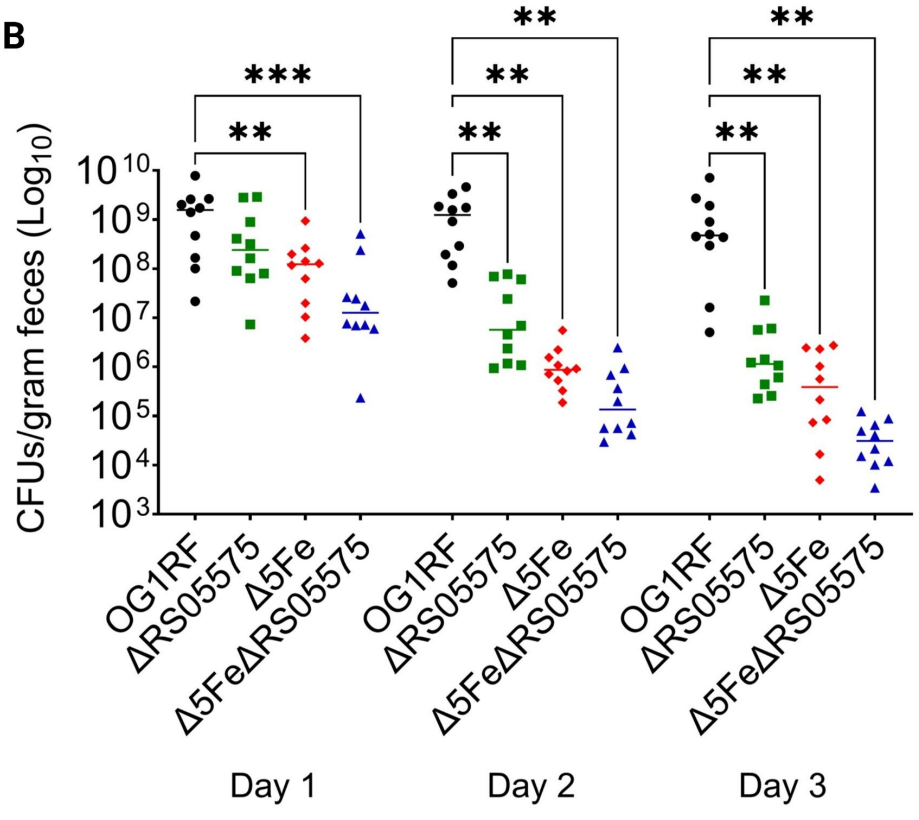
B
CFUs/gram feces (Log10)
10^10
10^9
10^8
10^7
10^6
10^5
10^4
10^3
***
**
**
**
**
**
**
OG1RF
ΔRS05575
Δ5Fe
Δ5FeΔRS05575
OG1RF
ΔRS05575
Δ5Fe
Δ5FeΔRS05575
OG1RF
ΔRS05575
Δ5Fe
Δ5FeΔRS05575
Day 1
Day 2
Day 3